Study of hybrid silicon quantum dot frequency comb laser dynamic for 5G and datacom applications

Bozhang Dong[1], Jianan Duan[1], Heming Huang[1], Geza Kurczveil[2], Di Liang[2], and Frédéric Grillot[1,3]
[1]*LTCI, Télécom Paris, Institut Polytechnique de Paris, 19 Place Marguerite Perey, 91120 Palaiseau, France*
[2]*Hewlett Packard Labs, 1501 Page Mill Rd, Palo Alto, CA 94304, USA*
[3]*Center for High Technology Materials, University of New-Mexico, Albuquerque, New-Mexico, 87106, USA*
e-mail: bozhang.dong@telecom-paris.fr

ABSTRACT

This work reports on the high performance of a 1.3 μm hybrid quantum dot frequency comb laser. The material parameters such as gain, differential gain, and linewidth enhancement factor are studied and linked to the comb dynamics. In particular, results show that a larger linewidth enhancement factor is more beneficial for comb operation; moreover, we demonstrate that, by employing optical injection, both the 3-dB bandwidth and the flatness of the whole optical frequency comb is improved. Such novel findings give promising guidelines for the development of high-speed dense wavelength division multiplexing photonic integrated circuits in upcoming 5G telecommunications and datacom applications.

Keywords: frequency comb, quantum dot, silicon photonics, optical injection, linewidth enhancement factor.

1 INTRODUCTION

Broadband optical light sources play a key role in the rapid development of wavelength-division multiplexing (WDM) technologies, which are solutions of high transmission capacity to meet the huge demand in the upcoming 5G telecommunication industry, next generation of data centers and LiDAR system applied to self-driving cars [1]. In contrast to the multiple single-wavelength lasers configuration, the multi-wavelength light source such as the optical frequency combs (OFCs) is therefore a competitive candidate for performing WDM functions, owning to the possibility to achieve a large number channels with equidistant free spectral range (FSR), which is able to support the huge demand in transmission capacity [2]; on the other hand, its reduced device footprint is also advantageous for photonic integrated circuits (PICs) applications. Quantum dot (QD) lasers have been found to be efficient solution to OFCs owning to straightforward comb generation, large gain bandwidth, narrow spectral linewidth, low relative intensity noise (RIN) and high temperature stability [3], [4]; hybrid semiconductor comb lasers fabricated on silicon substrate are developed as well to meet the requirement of low-cost and energy-efficient integrated photonic component for PICs. In this paper, we report on the improved performance of 1.3 μm hybrid QD comb lasers. To do so, we analyze the linewidth enhancement factor (α_H-factor) driven the coupling between gain and refractive index as well as the response of the comb laser to optical injection. The α_H-factor is known as a vital parameter influencing semiconductor laser performance. Then presented results show that the higher the reverse voltage applied on the saturable absorber (SA), the larger the α_H-factor, hence the stronger the frequency comb dynamics. With the view of improving the OFCs performance, we also demonstrate that optical injection (OI) is more beneficial to further enlarge the bandwidth and optimize the whole comb flatness.

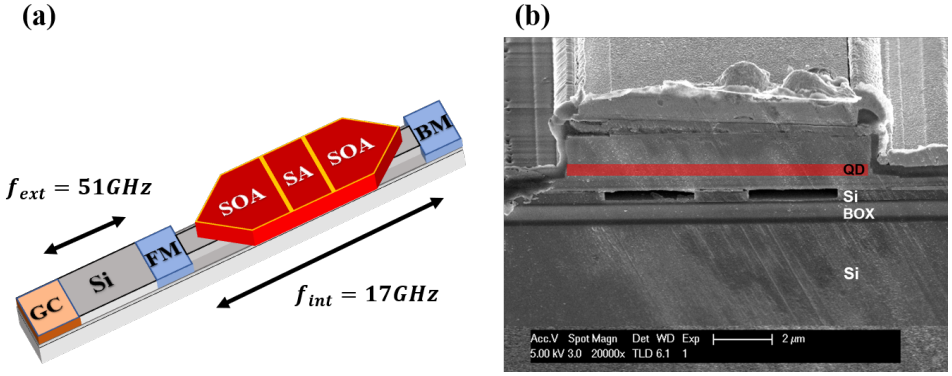

Figure 1. (a) Schematic diagram of the hybrid-silicon QD comb laser under study. SOA, semiconductor optical amplifier; SA, saturable absorber; FM, front mirror; BM, back mirror; GC, grating coupler. (b) SEM image of the cross section of the device. QD, quantum dot active region.

2 ANALYSIS OF DEVICE

2.1 Description of device

The schematic diagram and the SEM image of the hybrid-silicon QD comb laser is shown in Figure 1(a) and (b), respectively. The device under study consists of a 2.3-mm-long internal cavity (repetition rate at 17 GHz), where a 1200-μm-long semiconductor optical amplifier (SOA) and a 120-μm-long SA at the center are bonded. The two facets of the cavity are then combined with a front mirror (FM) and a back mirror (BM) at $\sim$50% and $\sim$100% power reflectivities, respectively. Outside the FM is followed by a 0.75-mm-long (repetition rate at 51 GHz) external cavity, which is applied to output a 102 GHz FSR on frequency comb behavior; and the light would eventually be coupled out by a $\sim$10% coupling efficiency grating coupler (GC). Varying the reverse voltage applied on the SA contributes to generate the comb dynamics, whereas the mode converters are applied to transfer the optical mode between the active hybrid waveguide and the passive Si waveguide. The full laser epitaxial structure and more detailed descriptions about the generation of 102 GHz repetition rate can be found elsewhere [5], [6].

2.2 Results discussions

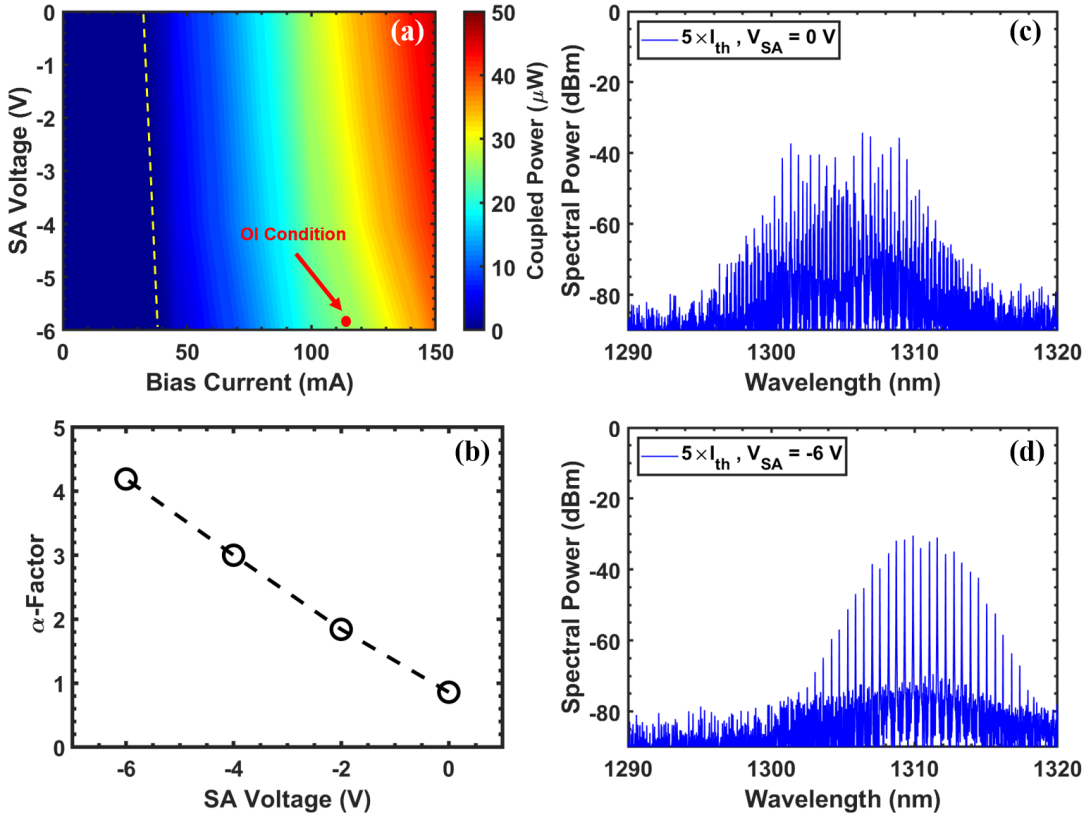

Figure 2. (a) Mapping of the coupled power under different reverse voltages on SA and bias current conditions. The yellow dashed line represents the evolution of the laser threshold with the reverse voltage. The red bullet corresponds to the device operation conditions applied in the optical injection, which is introduced in this paper hereafter. (b) α_H-factor at threshold as a function of reverse voltages on SA. Optical spectrum at $5\times I_{th}$ with reverse voltage on SA at (c) 0 V and (d) -6 V.

Figure 2(a) depicts the mapping of light - current characterization as a function of the reverse voltage on SA of the comb laser under study. Let us note that the device temperature is carefully monitored and kept constant at room temperature (293K) throughout the experiment. The evolution of threshold current I_{th}, which is marked by the yellow dashed line, indicates that a higher reverse voltage on SA decreases the output power and increases the threshold. For instance, I_{th} is found to slightly increase from 32 to 38 mA as the reverse voltage is varied from 0 V to -6 V, which is introduced by the higher internal loss from the increasing absorption in SA.

Not only the threshold and output power, but also the α_H-factor is found to vary from different reverse voltage applied on SA. In this section, the extraction of the LEF is performed from the amplified spontaneous emission (ASE) [7]. With the view of ensuring a better precision of the LEF extraction, we used a CW current source to get smooth optical modes, which would then be captured by a 20 pm high resolution optical spectrum

analyzer (OSA); on the other hand, the modal wavelength red-shift above threshold caused by thermal effects is then totally subtracted from the wavelength blue-shift below threshold. Both the operations leads to an accurate extraction of the LEF from below to threshold.

The extracted α_H-factors at threshold as a function of the reverse voltage on SA are shown in Figure 2(b). The values of α_H-factor are found to increase from 0.9 to 4.2 with the reverse voltage from 0 V to -6 V due to the increase of modal differential wavelength and the decrease of the differential gain. It should be noted that a larger α_H-factor is found to optimize the frequency comb dynamics, which can be clearly seen in Figure 2(c) and (d). This enlargement of comb bandwidth through four-wave mixing is attributed to the homogeneous broadening introduced by the spatial overlap among the quantum dots [8]. Nevertheless, let us stress that the increase of the comb bandwidth is limited because the dispersion for high frequency active mode is bigger. By the way, let us stress that the device under study does not output any pulse (no mode-locking) but rather operates under continuous-wave (CW) which is desired for WDM applications, as such devices are likely to have better reliability from the lower instantaneous power.

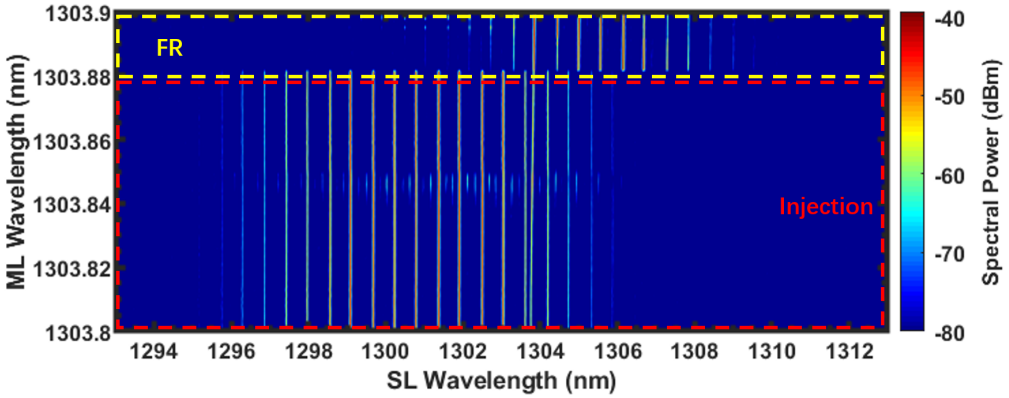

Figure 3. Evolution of the optical spectra of the slave comb laser as a function of the injected wavelength, device is biased at $3\times I_{th}$ with -6V applied on SA. Optical spectra at free running state are highlighted in the yellow dashed area (FR) and that under optical injection are in the red dashed area (Injection). ML, master laser; SL, slave laser.

With the view of improving the comb dynamics, we also investigated the effects of the OI as a way to process optical frequency comb by isolating and amplifying individual comb modes. The OI is applied when the device operates at $3\times I_{th}$ with -6 V applied on SA (conditions marked by red bullet in Figure 2(a)), and the injection strength is estimated to be below -12 dB. Let us stress that the α_H-factor is therefore considered as a constant and not being influenced by the injected field due to such low injection strength. Figure 3 displays the evolution of optical spectra of the slave comb laser by varying the injection wavelength of master laser, where the optical spectra at free running state (without OI) are marked by the yellow dashed area (FR) and that under OI are highlighted in the red dashed area (injection). Under the intramodal injection at the peak of 1303.8 nm, a stable blue-shift of the comb spectrum as well as a broadening of comb bandwidth are observed. In our case, the full bandwidth of the comb laser broadens from 5.7 nm (11 lines above noise floor) to 10.7 nm (20 lines above noise floor), and its 3-dB bandwidth enlarges from 1.1 nm (3 lines) to 4 nm (8 lines). Such findings bring novel insights in the optimization of frequency comb dynamics.

3 CONCLUSIONS

To summarize, this investigates the role of optical injection on the high-performance of a frequency comb laser. We link the comb dynamic to the material properties such as that driven by the α_H-factor. Therefore, a larger α_H-factor occurs at higher reverse voltage on SA which in principle contributes to strengthen the comb laser performance. Intramodal OI is also proved to enhance the bandwidth and flatness of the comb spectrum. Those novel findings are very encouraging for the future integrated technologies required for 5G telecommunications and supercomputer applications.

REFERENCES

[1] H. Ito et al., Opt. Express, Vol. 26, No. 20 (2018).

[2] H. Hu et al., Nat. Photon., vol. 12 (2018).

[3] Z. G. Lu et al., Opt. Express, vol. 26, 2160-2167 (2018).

[4] H. Huang et al., APL Photonics, Vol. 5, 016103 (2020).

[5] G. Kurczveil et al., IEEE Photon. Technol. Lett. Vol. 30, No. 1 (2018).

[6] B. Dong et al., Opt. Lett., Vol. 44, No. 23 (2019).

[7] J. Duan et al., Photonics Res., Vol. 7, No. 11 (2019).

[8] F. Grillot et al., IEEE J. Quantum Electron. Vol. 45, 872 (2009).